Phase diagram of the two-dimensional Anderson-Hubbard model

Jaichul Yi, Lizeng Zhang, and Geoff S. Canright
Department of Physics and Astronomy, University of Tennessee, Knoxville, Tennessee 37996-1200
and Solid State Division, Oak Ridge National Laboratory, Oak Ridge, Tennessee 37831
(Received 21 December 1993)

We study the ground state of the two-dimensional Anderson-Hubbard model using a quantum real space renormalization group method. We obtain the phase diagram near half filling. The system is always insulating with disorder. At half filling, the system undergoes a transition from a gapless (Anderson) insulator to an incompressible (Mott-Hubbard) insulator as the interaction U reaches a critical value U_c. Away from half filling, the insulating phase is always gapless and is found to be controlled by the Anderson fixed point at half filling. This result is similar to that obtained in the corresponding one-dimensional system and suggests strongly the importance of the electron-electron correlation in this gapless insulating phase.

I. INTRODUCTION

When disorder is introduced into a physical system, it will result in the localization of some single-particle states.[1] For a noninteracting electron system, if the states at the Fermi surface are localized, the system is a so-called "Anderson insulator." In reality, the interaction between electrons always exists, and such a single-particle picture may not apply. The understanding of the interplay between disorder and interaction has been an important issue in condensed matter physics.[2] This issue has become more interesting since the discovery of the high temperature superconductors.[3] On the one hand, it is commonly believed that these materials are strongly two dimensional (2D) in character, and that electron-electron correlations are important and are responsible for many of their unusual physical properties; on the other hand, it is also clear that disorder, which manifests itself as (e.g.) oxygen vacancies, is inevitably present in these materials. It is thus of interest to investigate the effect of disorder in highly correlated systems. In this paper, we pursue such a study using a real space renormalization group (RG) approach. The model we consider is the two-dimensional Anderson-Hubbard model defined by the Hamiltonian

$$H = \sum_{\substack{\langle i,j\rangle \\ \sigma}} (t_{ij} c_{i\sigma}^{\dagger} c_{j\sigma} + \text{H.c.}) + \sum_{i\sigma} (W_i - \mu) n_{i\sigma} + U \sum_i n_{i\uparrow} n_{i\downarrow}. \tag{1.1}$$

Here $c_{i\sigma}^{\dagger}$ ($c_{i\sigma}$) is the creation (annihilation) operator for a spin-σ electron on site i, t_{ij} is the nearest-neighbor intersite hopping energy, and U (> 0) gives the on-site Coulomb repulsion energy. The chemical potential is given by μ, and W_i is a random site potential which has an independent Gaussian distribution with zero mean and width W, i.e., $\overline{W_i} = 0$ and $\overline{W_i W_j} = W^2 \delta_{ij}$ (where the overbar indicates random average). We shall consider only the square lattice case. Without interaction ($U = 0$) but with disorder, this is the Anderson model[1] of localization which has been the prototype for studying the effect of disorder in electron systems. With interaction but without disorder ($W_i \equiv 0$), this is the Hubbard model,[4] which is believed to be one of the simplest theoretical models which possesses the essential physics of correlation,[5] and which has been the focus of intense theoretical investigation since the discovery of high-T_c superconductors. Thus, the Anderson-Hubbard model is a natural starting point for the investigation of the combined effects of disorder and interaction in electron systems. Throughout the paper our discussion will be restricted to ground-state properties; also, we will not consider the issue of magnetic ordering.

For the Anderson model in 2D, the consensus is that all of its eigenstates are localized, and hence that it describes a gapless insulating state.[2] For the Hubbard model at half filling, on the other hand, it is commonly accepted that the Coulomb repulsion U gives rise to insulating behavior, with long-ranged antiferromagnetic ordering in the ground state. Thus, in contrast to the usual "band insulator" where the insulating phase is due to the filling of electron bands in the solid, and different from the Anderson insulator where the vanishing conductivity is caused by the localization of the single-particle states at the Fermi surface, the insulating state in the Hubbard model at half filling is a result of electron-electron correlations, hence a "correlated insulator." Away from but close to half filling, the Hubbard model describes a highly correlated system whose exact properties we still know little about despite intense studies during the past few years. Candidates for the possible ground states can be, e.g., phase separation,[6] a highly correlated metal,[7] or a superconductor.[5,7] When both interaction and disorder are considered, one expects that disorder breaks the translation and other lattice symmetries and possibly weakens the effect of the correlations; on the other hand, strong correlations may render the standard single-particle picture of Anderson localization meaningless. As a first step towards understanding this complicated issue, we wish to identify the phase diagram of the 2D Anderson-Hubbard model.

Previously, the Landau Fermi-liquid idea has been employed to describe systems of weakly interacting electrons with (weak) disorder.[2] The validity of approaches along this line is questionable in the present situation because the noninteracting system is non-metallic, and because the effect of the interaction is presumably nonperturbative. The real space RG approach,[8–13] on the other hand, is a nonperturbative method which allows one to treat disorder and interaction of any strength on the same footing. It has however the disadvantage of being an uncontrolled approximation, so that its implementation and interpretation should be taken with extra caution.

The real space RG scheme adopted in this paper is a generalization of the works of Hirsch[8] and Ma.[9] This method allows one to study the compressibility of the system by investigating the renormalization of chemical potential and the corresponding flow of density. This RG scheme has been previously employed to study the $U = \infty$ Anderson-Hubbard model for spinless bosons.[11,12] While the quantitative results, such as the critical exponents of the superfluid–Bose-glass phase transition, are still the subject of some controversy,[14] this method does provide the correct qualitative physical picture. For instance, it shows that the superfluid phase is unstable against any amount of disorder in the 1D $U = \infty$ Anderson-Hubbard model, in agreement with the exact result;[15] in 2D and 3D, it shows a transition from the superfluid phase to a disordered (Bose-glass) phase at some critical amount of disorder, as indicated by other theoretical approaches.[14] Thus we have reasons to believe that the real space RG approach can also give us useful information concerning the fermion Anderson-Hubbard model (1.1). In addition, the validity of the real space RG scheme for the present case may be tested in the noninteracting system; for this case our method gives the result that the metallic phase is unstable against any amount of disorder (see below), consistent with the now accepted theoretical results.[2,16]

One may wonder why we are in a position to investigate the Anderson-Hubbard model when there is still not a good understanding of even the pure system. Our response to this question is that, as discussed previously,[11,12] and as will be emphasized in the section to follow, disorder is in fact an advantage for our investigation. By sampling a large ensemble of random configurations of the potential $\{W_i\}$, the problem of losing long-range quantum correlations due to breaking the system into blocks in the real space RG may be partially compensated. Also, the disorder averaging allows us to treat the (average) particle $\overline{n}$ as a continuous variable—which is not possible in the absence of disorder. Finally, even for disordered systems there already exist some known cases where one can test the method, as discussed above. These considerations give us some confidence that our real space RG approach to the disordered problem is a suitable choice, at least for our present purpose of investigating the phase diagram.

The rest of the paper is organized as follows: the real space RG method is described in some detail in the next section; in Sec. III, we present our results; and we offer a summary and discussion in Sec. IV.

II. METHOD

Our real space RG method is similar to that of Refs. 9 and 11. This real space RG is implemented numerically on a finite lattice. The random field $\{W_i\}$ is obtained through a Gaussian random number generator. Briefly, the RG procedure can be described in the following five steps: (i) Divide the lattice into blocks of size n_s. (ii) Compute the block fermion operators which are defined in terms of four eigenstates of the block Hamiltonian. Each block is characterized by an effective on-site potential and an on-site repulsion between the "block particles." (iii) Determine the hopping parameters for the block particles from the interblock couplings between the site variables. However, since the block parameters arise from the random $\{W_i\}$, and so have in general a different distribution from the original one, we need to (iv) repeat the above procedures [(ii) and (iii)] for a large random ensemble to determine the distribution of the block parameters. We shall limit ourselves to tracking only the first two moments of each distribution (see below). At this stage, the Hamiltonian is mapped back onto its original form with renormalized parameters

$$\widetilde{H} = \sum_{\substack{\langle\alpha\beta\rangle \\ \sigma}} (\tilde{t}_{\alpha\beta}\tilde{c}^{\dagger}_{\alpha\sigma}\tilde{c}_{\beta\sigma} + \text{H.c.}) + \sum_{\alpha\sigma}(\widetilde{W}_{\alpha} - \tilde{\mu})\tilde{n}_{\alpha\sigma} + \widetilde{U}\sum_{\alpha}\tilde{n}_{\alpha\uparrow}\tilde{n}_{\alpha\downarrow} + \text{const} , \tag{2.1}$$

where α and β are block indices. Finally, (v) we iterate the above sequence to find the flow and fixed point(s) of the RG.

Now we elaborate each of the above steps

(i) The blocks we used in the present work are shown in Fig. 1. Each of them is chosen to have an odd number of sites, to allow us to correctly treat the physics of half filling.[17] Even for such small blocks the numerical diagonalization is nontrivial, due to the large Hilbert space and the necessity of sampling a large number of random configurations. For the 3×3 square lattice at half filling, for instance, the dimension of the Hilbert space is 15 876×15 876. (Here the lattice symmetry is destroyed by disorder and thus cannot be used to reduce the size of the Hilbert space.) Both types of blocks shown in Fig. 1 have been tested, and we find that they give the same qualitative physics. Thus for our present purpose (exploring the phase diagram) we may focus on the "star" block [Fig. 1(a)] which is computationally more convenient.

(ii) Each (microscopic) site can have one of four possible states: the no-electron state $|0\rangle$, the up-spin electron state $|\uparrow\rangle$, the down-spin electron state $|\downarrow\rangle$, and the two-electron state $|\uparrow\downarrow\rangle$. The energy for the no-electron state is denoted $E^{(0)}$, and the two-electron state energy $E^{(2)}$. The up- and down-spin electron state energies are degenerate and denoted by $E^{(1)}$. For each block, we find the exact ground state and ground-state energy for the Hamiltonian [Eq. (1.1)] for every possible odd number of particles, restricted to the subspace with $S = \frac{1}{2}$ (the two $S_z = \pm\frac{1}{2}$ states are degenerate). The lowest energy

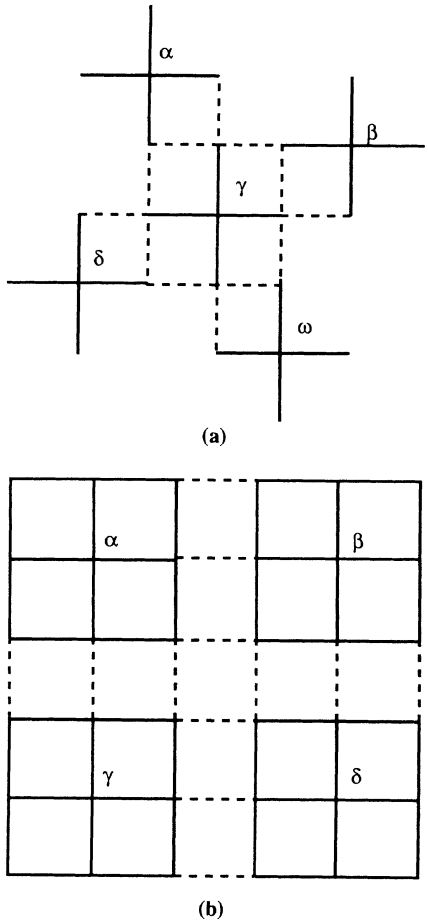

FIG. 1. Two types of blocks used in our RG approach for the square lattice. (a) Star lattice, (b) 3×3 lattice.

among these ground-state energies then gives us $E^{(1)}$. Letting N_α be the number of particles which gives $E^{(1)}$ in block α, and $|\uparrow_\alpha\rangle$ the corresponding ground state, we then take the $N_\alpha - 1$ ground state (from the subspace $S = 0$) as $|0_\alpha\rangle$ (with energy $E^{(0)}$), and the $N_\alpha + 1$ ground state ($S = 0$) as $|\uparrow\downarrow_\alpha\rangle$ (with energy $E^{(2)}$). The block variables may be determined from these states as follows:

$$U^\alpha = E_\alpha^{(2)} + E_\alpha^{(0)} - 2E_\alpha^{(1)} , \tag{2.2}$$

$$W^\alpha - \mu^\alpha = E_\alpha^{(1)} - E_\alpha^{(0)} . \tag{2.3}$$

(iii) The hopping energy between two neighboring blocks is obtained from the hopping energy of the neighboring sites on these two blocks. We calculate the matrix elements in the new states by insisting that those states are the same for both the new and the old Hamiltonians. There are four nonzero matrix elements for t for each bond between blocks α and β,

$$\tilde{t}_{\alpha\beta}^{(1)} = \langle 0_\alpha \uparrow_\beta | \tilde{H}_t | \uparrow_\alpha 0_\beta \rangle = \langle 0_\alpha \uparrow_\beta | H_t | \uparrow_\alpha 0_\beta \rangle , \tag{2.4}$$

$$\tilde{t}_{\alpha\beta}^{(2)} = \langle \uparrow_\alpha \downarrow_\beta | \tilde{H}_t | 0_\alpha \uparrow\downarrow_\beta \rangle = \langle \uparrow_\alpha \downarrow_\beta | H_t | 0_\alpha \uparrow\downarrow_\beta \rangle , \tag{2.5}$$

$$\tilde{t}_{\alpha\beta}^{(3)} = \langle \uparrow\downarrow_\alpha 0_\beta | \tilde{H}_t | \downarrow_\alpha \uparrow_\beta \rangle = \langle \uparrow\downarrow_\alpha 0_\beta | H_t | \downarrow_\alpha \uparrow_\beta \rangle , \tag{2.6}$$

$$\tilde{t}_{\alpha\beta}^{(4)} = \langle \uparrow\downarrow_\alpha \downarrow_\beta | \tilde{H}_t | \downarrow_\alpha \uparrow\downarrow_\beta \rangle = \langle \uparrow\downarrow_\alpha \downarrow_\beta | H_t | \downarrow_\alpha \uparrow\downarrow_\beta \rangle . \tag{2.7}$$

There are three bonds allowing hopping between any two star blocks α and β (also in the square blocks; see Fig. 1). We sum these three hops to get $\tilde{t}_{\alpha\beta}^{(i)}$. The above four $\tilde{t}_{\alpha\beta}$'s are then averaged, $\tilde{t}_b = \frac{1}{4}\sum_{i=1}^{4} \tilde{t}_{\alpha\beta}^{(i)}$, for one connection $\tilde{t}_b$ between two blocks α and β.

(iv) Now we average over an ensemble of random configurations to determine the distribution of the parameters in the block Hamiltonian. Since (2.2) is always positive (as verified numerically), we simply use its mean (denoted as $\widetilde{U}$) as the renormalized on-site repulsion between the block particles. The renormalized chemical potential $\tilde{\mu}$ is defined by the mean of the right hand side of (2.3). This implies that the renormalized random potential $\{W^\alpha\}$ has zero mean. However, the distribution of the block potential is in general different from the original one. Here we choose to keep track of only the first two moments, the mean ($\equiv 0$) and the variance ($\equiv \widetilde{W}$); we thus map the renormalized distribution of the $\{W_i\}$ back onto an (independent) Gaussian form.

The determination of the block hopping parameter is more subtle. Consider a block (of any size) without disorder. In general, the ground state is degenerate, where the degeneracy is related to the symmetry of the lattice and to the Fermi statistics of the electrons. Any amount of disorder breaks this lattice symmetry and therefore lifts the degeneracy. As (degenerate) perturbation theory shows, depending on the configuration of the random fields $\{W_i\}$, the sign of the $\tilde{t}_{\alpha\beta}$'s can be either positive or negative. This causes *frustration* when the product of $\tilde{t}_{\alpha\beta}$'s around a closed path is negative. This is different from the boson case considered in Ref. 11 where the ground state of the pure system is nondegenerate and the kinetic energy is unfrustrated by site disorder. To take this effect of frustration into account, one has thus to keep track of the lattice structure. More specifically, for the star block considered here, we first build a square lattice which consists of $n_b = 125$ coupled star blocks ($n_s \times n_b = 625$ sites). Step (iii) is then performed to obtain the corresponding block hopping parameters. This explicit lattice structure enables us to compute the frustration index (defined by the ratio of the number of frustrated plaquettes to the total number of plaquettes). It turns out that, starting from a uniform hopping constant $t_{ij} = t$, the RG described above will randomize the hopping parameter and frustrate the kinetic energy. Regardless of the starting configuration, the frustration index for the block system is always near 0.5. We approximate the block hopping parameters with an independent Gaussian distribution which is determined by their mean $\tilde{t}_{\rm av}$ and variance $\tilde{t}_{\rm var}$. In the actual calculation, we typically average over n_{sb} =5–10 such lattices. Due to the symmetry of the square lattice, one can always choose the mean of the hopping parameter $\tilde{t}_{\rm av}$ to be positive. Hence we take $\tilde{t}_{\rm av} = |\bar{t}|$ and $\bar{t} = (1/N_\alpha)\sum_{\substack{\text{disorder}\\ \langle\alpha\beta\rangle}} \tilde{t}_{\alpha\beta}$ with $N_\alpha = n_{sb} n_b$; the variance is then

$$\tilde{t}_{\rm var} = \left[\frac{1}{N_\alpha - 1} \sum_{\substack{\text{disorder}\\ \langle\alpha\beta\rangle}} (\tilde{t}_{\alpha\beta} - \bar{t})^2 \right]^{1/2} .$$

Under the RG iterations for the 2D problem, $\tilde{t}_{\rm av}$ decreases rapidly, reflecting the frustration.

(v) Using the new set of parameters one can repeat the process described above and study the flow of the parameters under the RG iteration. Physical phases are identified from the stable fixed points of the RG.

The Hamiltonian (2.1) is characterized by four independent parameters, which may be chosen as $\tilde{t}_{\rm av}/\widetilde{W}$, $\widetilde{U}/\widetilde{W}$, $\tilde{\mu}/\widetilde{W}$, and $\tilde{t}_{\rm var}/\widetilde{W}$. Among the others, $\tilde{t}_{\rm var}/\widetilde{W}$ is found to always renormalize to zero; hence we shall not discuss this parameter further in the following. For simplicity we label the relevant dimensionless parameters as follows: $\widetilde{U}/\widetilde{W} \equiv U/W$ gives the strength of the repulsion; the flow of $\tilde{t}_{\rm av}/\widetilde{W} \equiv t/W$ indicates insulating ($\to 0$) or metallic ($\to \infty$) behavior; and $\tilde{\mu}/\widetilde{W} \equiv \mu/W$ gives a dimensionless measure of the chemical potential.

The choice of the block states described in (ii) needs some more explanation. We truncate the Hilbert space of the block by choosing four low lying states such that the block Hamiltonian and the site Hamiltonian have the same form. However, there are different possibilities of choosing these four states. The simplest possibility (implemented in Ref. 9 at half filling) is always to pick the same $N_\alpha = N$ for every block α. This "fixed-n" (where n is defined by $n \equiv N_\alpha/n_s$) procedure is the most artificial of the procedures we have used; however, one might argue that it is adequate for incompressible states.

A second ("fixed-μ") procedure is to fix the chemical potential μ rather than the density n. This procedure can only work, however, if the chosen value for μ corresponds to a density which can be represented on the blocks by an integer particle number; otherwise, instabilities occur in the RG flow.[11] Hence we have only used the fixed-μ procedure at half filling. In this case, the chemical potential is known to be precisely $U/2$ and can therefore be set at the beginning of the RG iteration. Since the distribution of the random potential $\{W_i\}$ is symmetric with zero mean, the statistical fluctuations will then preserve the average density at 1 and $\tilde{\mu}$ at $\widetilde{U}/2$ by averaging over the random configurations. Since the density is allowed to vary from block to block, this method allows one to study compressible as well as incompressible states.

The possibility of allowing the density to fluctuate in such a real space RG scheme is unique to disordered systems. In a pure system, all blocks are identical and N_α will thus be chosen the same for all blocks. The particle number fluctuation in any given region (of any size) is thus 1, so that the RG can only describe an incompressible state.[11] Thus one expects that such a real space RG scheme for pure systems will be mostly applicable at half filling, where it is indeed incompressible.[18]

We have used a third procedure to study the physics in a region around half filling, by allowing the chemical potential to flow also in the RG iterations. This enables us to explore the RG flow in the full 3D parameter space $(t/W, U/W, \mu/W)$. In the absence of disorder, this would not be possible, since the density cannot vary in any block. In the presence of disorder, one selects N_α which minimizes the energy in a given block α, and thus allows $\overline{n}$ (where again the overbar means disorder average) to vary continuously along with μ. However this flow must fail at high and low densities, where the small size of our blocks imposes strict upper and lower bounds on the range of densities which can be handled by the method—for example, the density in a star block cannot fall below 0.2 nor exceed 1.8. Hence with this procedure it is necessary to follow the flow of $\overline{n}$ as well, and to discard flows when $\overline{n}$ saturates at its upper or lower bound. With this procedure it is sometimes convenient to parametrize the chemical potential as $\tilde{\mu}/\widetilde{U} \equiv \mu/U$ since it is in terms of this parameter that we can locate half filling ($\overline{n} = 1$ at $\mu/U = 1/2$).

III. RESULTS

We start by considering the Anderson model ($U = 0$). In this case, with either the fixed-n or the fixed-μ method, the only meaningful parameter of the system is t/W. Either procedure gives the same qualitative result: we find two fixed points, at $t/W = 0$ and at $t/W = \infty$. The fixed point describing the pure system ($t/W = \infty$) is unstable, with flow towards the attractive (insulating, $t/W = 0$) fixed point. Thus we find that, for noninteracting fermions, disorder is always relevant, in agreement with the prediction from scaling theory.[16,19]

Next we consider the interacting case $U \neq 0$. In Fig. 2, we show RG flow diagrams in the two-dimensional parameter space $(t/W, U/W)$. Figure 2(a) is obtained at half filling. Here we again find that the two RG procedures (fixed n and fixed μ) give similar results. Figure 2(b) depicts RG flow at densities away from half filling, obtained using the fixed-n procedure. The possible densities are $n = 1/5, 3/5$ for the star blocks, and

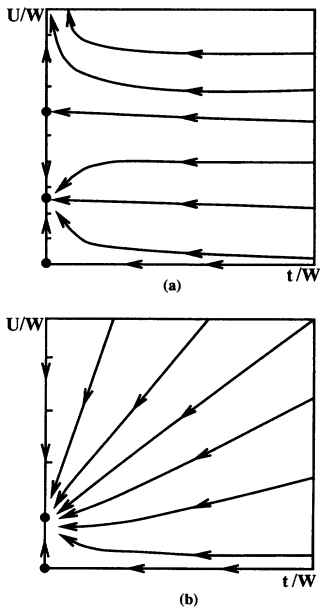

FIG. 2. Flow diagrams of the 2D Anderson-Hubbard model as obtained by our RG approach, at fixed filling of the lattice. (a) For half filling we see two insulating phases: a Mott-Hubbard phase at large U/W and an Anderson (gapless) phase at smaller U. (b) Away from half filling we see only the Anderson phase.

$n = 1/9, 3/9, 5/9, 7/9$ for the 3×3 square blocks (apart from those which may be obtained using particle-hole symmetry). They all give qualitatively the same flow diagrams. At half filling, Fig. 2(a) shows that, apart from the unstable fixed points describing the noninteracting ($U = 0$) and pure ($t/W = \infty$) phases, there are two stable fixed points at ($t/W = 0, U/W = \infty$) and at ($t/W = 0, U/W \approx 1.3$). Between these two phases is a separatrix which terminates at a repulsive fixed point [$t/W = 0$, $U/W = (U/W)^* \approx 7.3$]. Away from half filling and at fixed density, the RG flow has only one stable fixed point, at finite U/W. We note that, with respect to the noninteracting system, U is relevant at all the fillings we examined.

We next ask, what is the nature of the various phases revealed by the stable fixed points in Fig. 2? Since t/W renormalizes to zero in all the cases, there is no metallic state. However, the nature of the insulating states needs some elaboration. We consider first the half-filled case. For the pure system (Hubbard model) at half filling, it is believed that the system is always insulating with long-ranged antiferromagnetic order for any finite $U > 0$. However, while the disordered system is always insulating, the physics responsible for the insulating behavior may vary. This situation is best illustrated in the essentially exact calculations on the infinite-dimensional Hubbard model:[20] at low but above the Néel temperature, there is a critical value of $U = U_c$, beyond which a gap opens up in the quasiparticle spectrum and the system changes from a metal to a Mott-insulating state. Such a paramagnetic solution persists down to $T = 0$, although it becomes unstable at low temperature and the true ground state is antiferromagnetic for any finite value of U. Thus one may expect that, while for small U the insulating state is a result of the delicate (antiferromagnetic) correlations, at large U it is simply due to the large energy cost for double occupancy. Upon introducing disorder, the Mott transition (masked by the antiferromagnetic long-range order in the pure case) is revealed, but the corresponding metallic state now becomes insulating also. Hence we interpret the state described by the fixed point at $(U/W) \to \infty$ as the Mott-Hubbard phase, while that associated with the fixed point at finite U/W we will call the "Anderson" phase, since it is expected (to be corroborated below) to be gapless.

Remarkably, this phase diagram is quite similar to that for the 1D case, which was calculated at half filling in Ref. 9 using the fixed-n method. (We have obtained the same picture for the 1D Anderson-Hubbard problem using the fixed-μ method at half filling.) The value of the unstable fixed point separating the two insulators is about $(t/W, U/W)^* \cong (0, 7.3)$. This value for the 2D system is very close to the fixed point obtained by Ma for the 1D case [$(t/W, U/W) = (0, 8.3)$], and to the slope of critical line for the opening of a compressibility gap in the (U_c, W) plane obtained by Domínguez and Wiecko (DW)[21] for the 3D case, $U_c \cong 6.7W$ ($W/t \to \infty$). As mentioned before, in getting the hopping parameter $\tilde{t}_b$ between two blocks, we take an arithmetic average over four $\tilde{t}_{\alpha\beta}$'s to take account of frustration. The $\tilde{t}_{\alpha\beta}$'s tend to be of varying sign (for reasons discussed earlier) and hence to cancel each other when we average, so that the parameter t/W rapidly approaches zero as the RG iteration proceeds. The slope of the separatrix between the two insulators is, therefore, nearly zero (unlike the 1D case[9]).

The stable fixed point found (with fixed density) away from half filling can be interpreted naturally as a fixed point describing the Anderson insulating phase. Although this phase diagram is obtained using the RG procedure for fixed n—which is more appropriate for incompressible states—we believe that this Anderson phase is actually compressible from the physical point of view. The compressibility of this phase at or near half filling may be investigated through the RG flow in the 3D parameter space $(t/W, U/W, \mu/W)$.

We have studied the compressibility in our numerical RG calculations using two methods. One, which is purely heuristic, is to stop the calculation after a single iteration, associating the renormalized values of density and chemical potential with the (fixed) values of U, t, and W which were input. This method—which cannot probe the long-wavelength physics seen from repeated RG iterations—nevertheless gives surprisingly good results, possibly due to the large size (625 sites) of the finite lattice which we used, coupled with the further averaging over disorder. Results obtained using this method are plotted in Fig. 3. We see that (thanks to the disorder and the averaging) the density $\bar{n}$ flows smoothly with the chemical potential, with two significant exceptions. One exception occurs when the density *saturates* at the maximum or minimum value allowed by the finite size of our block (i.e., for the star block, 0.2 and 1.8). This saturation

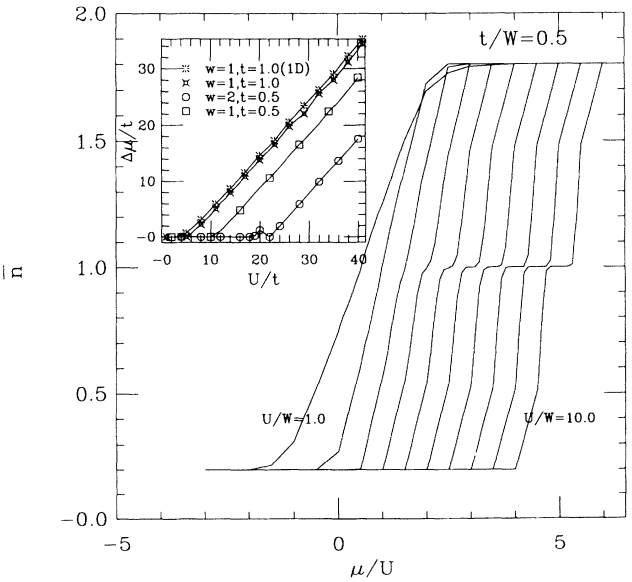

FIG. 3. Density versus μ/U with different U/W for fixed t (= 0.5) and W (= 1.0). Each curve is shifted to the right, for visual purposes, by 0.5 as U/W is increased by 1. Density is pinned at $\bar{n} = 1$ over a finite range in μ as U is increased. Inset: The incompressibility $\Delta\mu$ in the Mott-Hubbard phase is plotted as a function of U in units of t, for fixed W and t. For comparison, we include some results for the 1D lattice.

marks a limit beyond which our method gives meaningless results. The other departure from smoothness occurs at $\overline{n} = 1$, for sufficiently large U, and is due to the above-mentioned incompressibility. The incompressibility (the Hubbard gap) is broadened with increasing Coulomb repulsion (Fig. 3). In the inset we plot the Hubbard gap $\Delta\mu/t$ as a function of U/t, with fixed t and W. We can see that the Hubbard gap increases linearly with U. The slope α $[\equiv \frac{d(\Delta\mu)}{dU}|_t]$ of the three curves is about $\alpha \sim 1.0$, which is consistent with what is expected, and also with the result obtained by DW.[21]

From the inset of Fig. 3 we can write $\Delta\mu = \alpha(U - U_c)$ at fixed W. Then in $(\mu/U, U/W)$ parameter space the gap can be described (for fixed t) by

$$\frac{\Delta\mu}{U} = \alpha\left(1 - \frac{U_c}{U}\right) \quad \text{for} \quad (U \geq U_c). \tag{3.1}$$

Taking the large-U limit, the gap $\Delta\mu/U$ will approach α in μ/U and U/W space. Hence our second method for studying the behavior of the incompressibility is to follow the RG flow in the 3D parameter space $(t/W, U/W, \mu/U)$, distinguishing however those flows which remain pinned at $\overline{n} = 1$ from those which do not. Figure 4 is a 3D flow diagram inside the limits at which the density saturates, but projected out onto the 2D plane $(U/W, \mu/U)$. (We project out the behavior of t/W since it is the most predictable, always flowing to zero.) In this figure we see that the Mott-Hubbard phase (shown by the shaded area) with $\overline{n} = 1$ is bounded by Eq. (3.1). We can also see the two fixed points in the plot, which correspond to those in Fig. 2(a). For $U/W \to \infty$ we have a "fixed bar" (i.e., a *line* of fixed points in μ–t–U space) which attracts the flows inside the Mott-Hubbard phase. (This fixed bar is of course a fixed *point* in n–t–U space, with $n = 1$.) In the Anderson phase we can see that the parameter μ/U flows to the value for half filling $\mu/U = 1/2$. Hence we find that there is a finite region in density, around $\overline{n} = 1$, in which the system is a compressible (Anderson) insulating phase and is characterized by the fixed point at half filling.

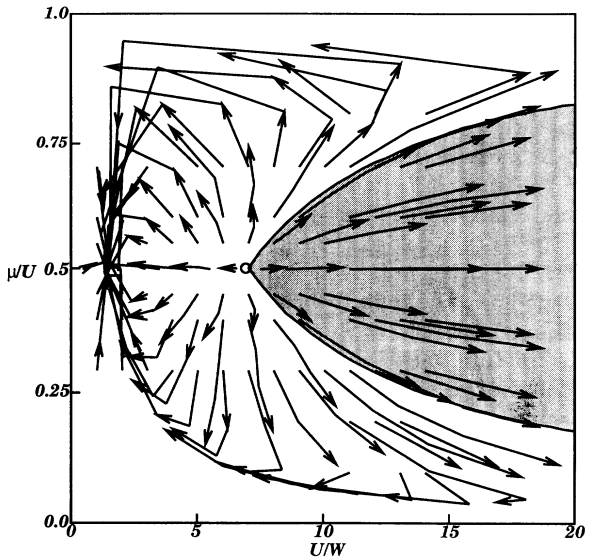

FIG. 4. Projection on a plane of flows of 3D RG parameters $\{t/W, U/W, \mu/U\}$. In our projection the flow of t/W is not shown, since this parameter always flows to zero. The Mott-Hubbard phase (in which the density is pinned at 1) is shaded. The unstable fixed point ($U/W = 7.3$, $\mu/U = 0.5$) marking the boundary of the Mott-Hubbard phase is marked with a small circle; the stable one is located at $(U/W, \mu/U) = (1.3, 0.5)$.

Since the discovery of high-T_c superconductivity, there have been suggestions that the dimensionality alone will invalidate the Fermi-liquid theory and make a 2D interacting system a highly correlated one,[22] as it does for its 1D counterpart. While for the 2D Hubbard model near half filling there is little doubt that the system is indeed highly correlated, controlled perturbative expansions suggest that at low density a system of interacting 2D fermions can be well described by the conventional Fermi-liquid theory.[23] If this is the case, the insulating state at low density would be simply due to the localization of the quasiparticles. From this point of view, one would expect that the (compressible) insulating state near half filling will be quite different from that at low (or high) densities, so that there should be an additional stable fixed point describing such a "conventional" Anderson insulating state, distinct from the "highly correlated" Anderson insulating state controlled by the fixed point at half filling. Hereafter we shall call the "conventional" Anderson phase an "Anderson-Fermi" insulator; the (presumably) highly correlated Anderson phase described by the Anderson fixed point at half filling we call the "Anderson-Luttinger" insulator. We choose the latter name since our RG study shows a strong resemblance between the 1D and 2D systems near half filling, and since generic (pure) 1D systems are described by the highly correlated Luttinger liquid.[24] In our studies we have found no evidence for an Anderson-Fermi insulating phase characterized by a high- or low-density fixed point.

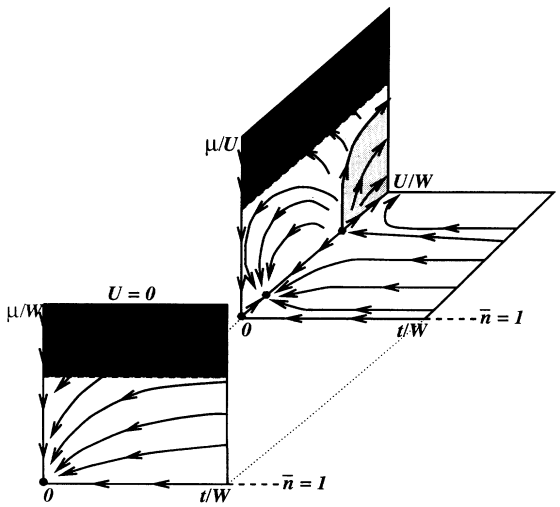

FIG. 5. 3D parameter flow diagram. In the dark area, where the density is saturated and so our method gives no information, we are assuming the chemical potential flows toward half filling. The Mott-Hubbard phase is marked with light shading.

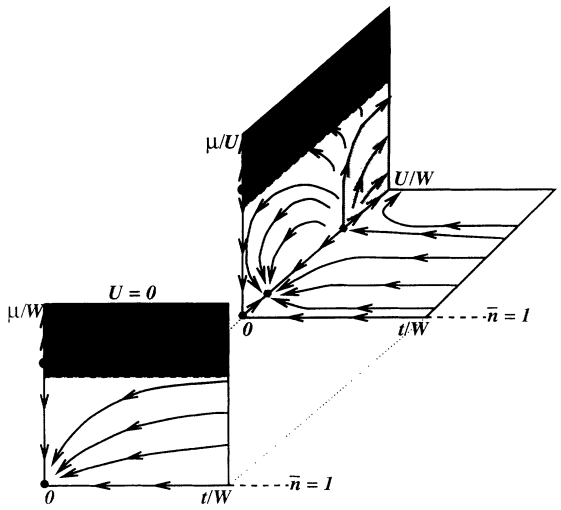

FIG. 6. 3D parameter flow diagram, but with an alternative hypothetical scenario from that shown in Fig. 5. Here we assume the existence of attractive fixed points in the dark areas (high and low density), indicating the presence of "uncorrelated" insulating phases distinct from the "correlated" phase we find around half filling. Since our method fails in the dark shaded area, it cannot distinguish between the picture shown here and that in Fig. 5.

We note however that we cannot rule out the existence of such fixed points, since our method is only reliable in a finite range of densities around half filling, and so may be incapable of detecting these uncorrelated phases.

In Fig. 5 and Fig. 6 we show the full flow diagrams in the 3D parameter space. Taking account of particle-hole symmetry, we omit the region $\overline{n} < 1$. We also omit $U < 0$ (which is expected to give different physics) and $t < 0$ which is trivially related to $t > 0$; hence we are left with one octant of the full space. In each plane the flows are the projection of 3D parameter flows. The incompressible Mott-Hubbard phase is lightly shaded in the $(\mu/U, U/W)$ plane. Our RG approach fails in a high- and a low-density region; the former is shown in Figs. 5 and 6 with dark shading. In this dark region we can imagine either two fixed points (one in the high-density region and the other one in the low-density area), or none. In the case of no fixed points in the dark area (Fig. 5)— or if the noninteracting fixed points are unstable to any finite U—the RG parameters outside the Mott-Hubbard phase flow to the one fixed point, so that there is only one ("correlated") Anderson phase in the Anderson-Hubbard model. On the other hand, if there are two stable fixed points (at high and low density) (Fig. 6), the Anderson-Hubbard problem will have two different Anderson phases as discussed above. We include both Figs. 5 and 6 because we do not believe that we can distinguish these two scenarios within the limitations of our method.

IV. SUMMARY AND DISCUSSION

Using a quantum real space renormalization group method, we have obtained the phase diagram of the 2D Anderson-Hubbard model near half filling at $T = 0$. A test of our method for noninteracting fermions shows the instability of the metallic phase for any nonzero disorder W, in agreement with commonly accepted results and hence providing some evidence that our method is qualitatively reliable. By studying the renormalization of chemical potential and the corresponding flow of particle density, we were able to estimate the compressibility gap $\Delta\mu$ in the Mott-Hubbard phase as a function of U and W. We found that $\Delta\mu$ increases proportional to the interaction U (at constant W) above a critical value $(U/t)_c$, with the constant of proportionality α about 1, and that $\Delta\mu$ decreases with increasing W (at fixed U). Our results here are also in good agreement with those obtained by other methods, which gives us further confidence in our approach.

Our studies show that there is no metallic phase for the 2D Anderson-Hubbard model, for any finite value of the random potential W and of the repulsive interaction U between the electrons. The interplay between interaction and disorder yields two insulating phases at half filling: an incompressible Mott-Hubbard insulator and a gapless Anderson insulator. The phase diagram strongly resembles that for the corresponding 1D system. Away from half filling, the insulating phase is always gapless, and its properties are controlled by the fixed point describing the Anderson insulator at half filling. We characterize such a highly correlated insulating phase as the Anderson-Luttinger insulator. U is relevant with respect to the noninteracting fixed point for all the cases we have considered. We would like to emphasize, however, that the relevance of U itself does not constitute evidence for the existence of the Anderson-Luttinger insulator. Since the noninteracting disordered system is described by the localized $(t/W = 0)$ fixed point, one may expect that, at least in the low-doping (near half filling) case, any interaction will be relevant regardless of the properties of the corresponding pure system, although there is a possibility that short-ranged interactions such as the on-site U studied here are not relevant in the dilute (low or high density) limit. The dilute fixed point, which presumably describes the conventional Anderson-Fermi insulator whose physics is related to that of localized noninteracting fermions has not been found within our approach, which is however limited to a range of densities around half filling.

The picture that we find at half filling is not unexpected: the instability of the noninteracting fixed point, the consequent finite-U (gapless) fixed point, and the opening up of a gap at U_c with flow towards $U = \infty$ in the Mott-Hubbard phase. The one feature of our results that is perhaps somewhat unexpected is the existence of a finite region in n (or μ) around half filling, which is dominated by the $n = 1$ fixed point. One could imagine a different result, namely, that, like the Mott-Hubbard phase, the Anderson-Luttinger phase is well defined only at or close to half filling, becoming unstable as n deviates from this region and flowing towards a dilute fixed point. In other words, one could imagine that $\delta\mu \equiv \mu - U/2$ is relevant when its magnitude becomes nonzero or sufficiently large, which is not what we have found for the

region allowed by our RG scheme.

It is conceivable that this result might be due to an artifact of our method. That is, one might conjecture that the flow towards half filling reflects only the stability of the *algorithm* at half filling, rather than the stability of the thermodynamic phase. Although we see no reason for this to be the case, we cannot rule out this possibility. We do however gain some confidence in the results of our RG method, in the case where we allow the chemical potential to flow, from the good agreement of these results for the Hubbard phase with existing results obtained by other methods. We note that these results (Figs. 3 and 4) were all obtained using this algorithm.

We therefore assume that the correlated Anderson-Luttinger insulator indicated by our results is in fact the true ground state of the 2D Anderson-Hubbard problem for some region around half filling. This suggests a number of directions for future work. It is clearly important to try to clarify the nature of this phase, in both the 2D and the 1D problems, for instance by calculating density-density or magnetic correlation functions and their RG flow. Furthermore, if indeed the physics for this disordered problem around half filling is described by the Anderson fixed point at half filling, one can expect to gain significant information about the lightly doped case by directly studying the half-filled case (where, for instance, there is no "sign problem" in quantum Monte Carlo simulations). It would also be of considerable interest to extend this work to the 3D problem, where one expects a metallic phase, and metal-insulator transitions of various types.[9] Unfortunately, the smallest isotropic 3D block with an odd site number $(3 \times 3 \times 3)$[17] is far too large for exact diagonalization. Since the 3-(spatial)-D problem is of interest both in its own right, and as a further test of the present 2D results, we believe that the problem of extending our real space RG technique for disordered systems to the 3D case merits some further effort. Finally, the issue of stability of long-range antiferromagnetic ordering (against potential disorder $\{W_i\}$) and the effect of disorder on magnetic properties, which are presumably important in the weak disorder regime and are not considered in the present work (since our RG procedure does not probe the pure limit), should be addressed in future investigations.

ACKNOWLEDGMENTS

We thank M. Ma and M. Randeria for useful discussions and comments. This research was supported by the NSF under Grant No. DMR-9101542, and by the U.S. Department of Energy through Contract No. DE-AC05-84OR21400 administered by Martin Marietta Energy Systems Inc. Part of the computations were carried out on the MASPAR MP-2 computer located at the University of Tennessee; we thank Christian Halloy of the Joint Institute for Computational Science (JICS) for help in the use of the MP-2.

[1] P. W. Anderson, Phys. Rev. **109**, 1492 (1958).
[2] See, e.g., P. A. Lee and T. V. Ramakrishnan, Rev. Mod. Phys. **57**, 287 (1985), and references therein.
[3] J. G. Bednorz and K. A. Müller, Z. Phys. B **64**, 188 (1986).
[4] J. Hubbard, Proc. R. Soc. London Ser. A **276**, 238 (1963); **277**, 237 (1964); **281**, 401 (1964).
[5] P. W. Anderson, Science **235**, 1196 (1987).
[6] V. J. Emery, S. A. Kivelson, and H. Q. Lin, Phys. Rev. Lett. **64**, 475 (1990).
[7] See, e.g., *High Temperature Superconductivity*, edited by K. S. Bedell *et al.* (Addison-Wesley, Reading, MA, 1990), and references therein.
[8] J. E. Hirsch, Phys. Rev. B **22**, 5259 (1980).
[9] M. Ma, Phys. Rev. B **26**, 5097 (1982).
[10] P. A. Lee, Phys. Rev. Lett. **42**, 1492 (1985).
[11] L. Zhang and M. Ma, Phys. Rev. B **45**, 4855 (1992).
[12] L. Zhang and X. Q. Wang, Phys. Rev. B **47**, 11 518 (1992).
[13] K. G. Singh and D. S. Rokhsar, Phys. Rev. B **46**, 3002 (1992).
[14] M. Ma, B. I. Halperin, and P. A. Lee, Phys. Rev. B, **34**, 3136 (1986); M. P. A. Fisher, P. B. Weichman, G. Grinstein, and D. S. Fisher, *ibid.* **40**, 546 (1989); K. Runge, *ibid.* **45**, 13 136 (1992); E. S. Sorensen, M. Wallin, S. M. Girvin, and A. P. Young, Phys. Rev. Lett. **69**, 828 (1992); M. Makivic, N. Trivedi, and S. Ullah, *ibid.* **71**, 2307 (1993).
[15] L. Zhang and M. Ma, Phys. Rev. A, **37**, 960 (1988).
[16] E. Abrahams, P. W. Anderson, D. C. Licciardello, and T. V. Ramakrishnan, Phys. Rev. Lett. **42**, 673 (1979).
[17] Blocks with an even site number n_s can also be employed with our method. However, since there is no odd N such that $n \equiv N/n_s = 1$ in the corresponding pure system, one would not find the Mott-Hubbard phase in this case. [The importance of odd N in our method arises from the Fermi statistics, as explained in step (ii) in the text.]
[18] J. Perez-Conde and P. Pfeuty, Phys. Rev. B **47**, 856 (1993).
[19] F. Wegner, Z. Phys. B **35**, 207 (1979).
[20] M. Jarrell and Th. Pruschke, Z. Phys. B **90**, 187 (1993); A. Georges and W. Krauth, Phys. Rev. B **48**, 7167 (1993).
[21] D. Domínguez and C. Wiecko, Phys. Rev. B **47**, 10 888 (1992).
[22] P. W. Anderson, Phys. Rev. Lett. **64**, 1839 (1990).
[23] J. R. Engelbrecht and M. Randeria, Phys. Rev. Lett. **65**, 1032 (1990); J. R. Engelbrecht, M. Randeria, and L. Zhang, Phys. Rev. B **45**, 10 135 (1992); H. Fukuyama, Y. Hasegawa, and O. Narikiyo, J. Phys. Soc. Jpn. **60**, 2013, 1991.
[24] V. J. Emery, in *Highly Conducting One-Dimensional Solids*, edited by J. T. Devreese, R. P. Evrard, and V. E. van Doren (Plenum, New York, 1979), p. 247; F. D. M. Haldane, J. Phys. C **14**, 2585 (1981).

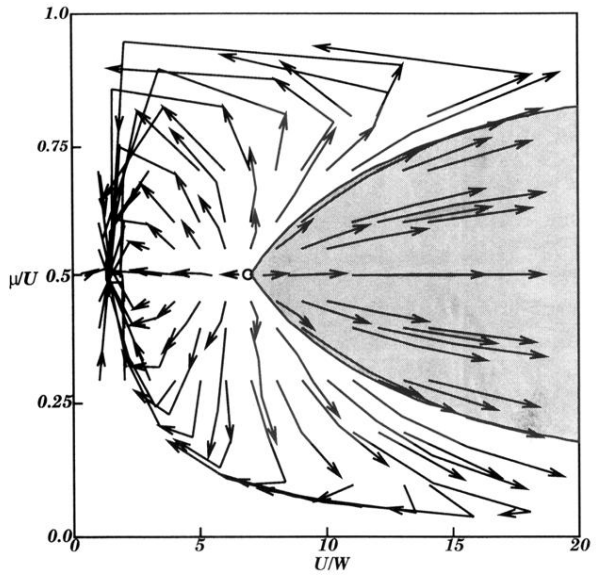

FIG. 4. Projection on a plane of flows of 3D RG parameters $\{t/W, U/W, \mu/U\}$. In our projection the flow of t/W is not shown, since this parameter always flows to zero. The Mott-Hubbard phase (in which the density is pinned at 1) is shaded. The unstable fixed point ($U/W = 7.3$, $\mu/U = 0.5$) marking the boundary of the Mott-Hubbard phase is marked with a small circle; the stable one is located at $(U/W, \mu/U) = (1.3, 0.5)$.

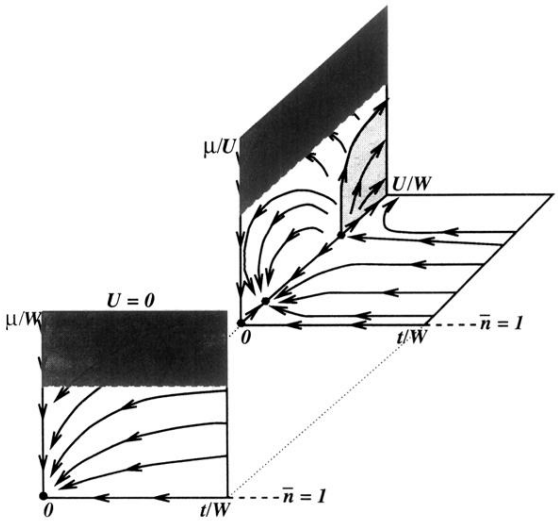

FIG. 5. 3D parameter flow diagram. In the dark area, where the density is saturated and so our method gives no information, we are assuming the chemical potential flows toward half filling. The Mott-Hubbard phase is marked with light shading.

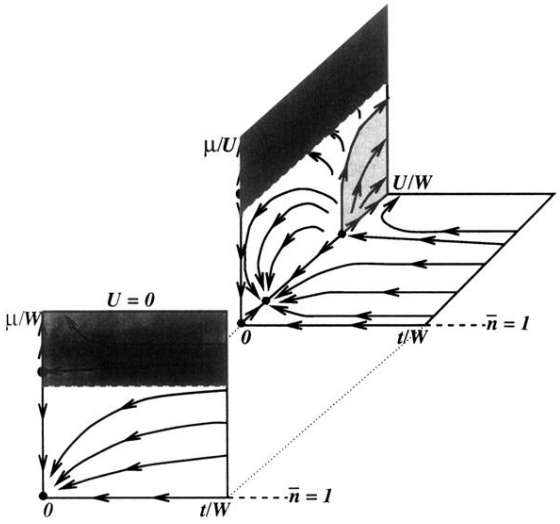

FIG. 6. 3D parameter flow diagram, but with an alternative hypothetical scenario from that shown in Fig. 5. Here we assume the existence of attractive fixed points in the dark areas (high and low density), indicating the presence of "uncorrelated" insulating phases distinct from the "correlated" phase we find around half filling. Since our method fails in the dark shaded area, it cannot distinguish between the picture shown here and that in Fig. 5.